J Mater Sci (2008) 43:4143–4151
DOI 10.1007/s10853-007-2166-9

REES RAWLINGS FESTSCHRIFT

Production of sintered materials from air pollution control residues from waste incineration

C. Dimech · C. R. Cheeseman · S. Cook ·
J. Simon · A. R. Boccaccini

Received: 28 June 2007 / Accepted: 13 September 2007 / Published online: 3 April 2008

Abstract Air pollution control residues from waste incineration have been washed to remove excess chloride and other soluble salts and blended with combinations of soda lime glass and waste electrostatic precipitator dust containing boric oxide from the fibre-glass industry. Homogenous fine powder mixes have been pressed and sintered at temperatures between 900 and 1000 °C. The physical properties and microstuctural characteristics of the glass–ceramics formed have been assessed. The results show that it is possible to produce a dense glass–ceramic material containing wollastonite and gehlenite crystalline phases with a hardness of 4.5 GPa. The high density and hardness means that the glass–ceramic may have a potential use in high value construction products.

Introduction

Changing waste management legislation in the UK and Europe is causing increasing amounts of municipal solid waste (MSW) to be disposed of by incineration in energy from waste (EfW) facilities. As increasing numbers of incinerators become operational the disposal of solid residues from these plants becomes an increasingly important issue [1]. Air pollution control (APC) residues are produced from the flue gas cleaning processes, and they are classified as hazardous waste in the European Waste Catalogue (19 01 07*) primarily due to high alkalinity, although they also contain heavy metals, dioxins and furans and other trace organics, and high levels of soluble salts including chlorides that are readily leachable and have potential to pollute soil, ground and surface waters [2–5]. APC residues must be treated prior to landfilling to meet leaching limits defined by the Waste Acceptance Criteria (WAC).

Current UK incineration capacity produces approximately 128,000 tonnes per annum of APC residues from approximately 80 plants. These include many smaller, company-specific incinerators, and by far the majority of APC residues, approximately 95% of the total, are generated from around 20 large EfW plants. Clinical waste incineration produces approximately 10,000 tonnes per annum and sewage sludge incineration a further 3,500 tonnes per annum. An additional 40,000 tonnes per annum of APC residues is expected to be generated from new UK MSW incineration capacity in the next few years.

A number of possible treatments have been investigated for the stabilisation and subsequent disposal of APC residues. These include the use of cementitious binders and the exploitation of the low compressive strength generated when APC residues are mixed with water [6–8]. However, the mobile soluble salt fractions and in some cases heavy metals are only partially immobilised within a cement matrix [6, 7, 9].

Washing of APC residues to remove problematic mobile fractions such as the chloride salts has been investigated by a number of researchers [10–13]. Although a large proportion of the soluble phases are readily removed, the resulting wash water generated represents a disposal problem.

C. Dimech · A. R. Boccaccini (✉)
Department of Materials, Imperial College London,
London SW7 2BP, UK
e-mail: a.boccaccini@imperial.ac.uk

C. R. Cheeseman
Department of Civil and Environmental Engineering,
Imperial College London, London, UK

S. Cook · J. Simon
Rio Tinto, London, UK

High-temperature thermal treatments such as sintering and vitrification to produce glasses and glass–ceramics from wastes are well-established technologies that can be used to produce inert and potentially reusable materials [6, 7, 14, 15]. These processes have been applied to many types of silicate wastes with a wide range of chemical compositions including coal fly ash [16, 17], wastes from mining and quarrying, e.g. borates, gold and slate wastes [18–20], metallurgical waste from zinc and steel processing [21, 22], waste glass [23] and bottom ash and fly ash from municipal waste incinerators [24–28]. However the application of thermal treatment methods on APC residues has not been reported in detail, with few reports available in the literature [29–31].

APC residues from a waste-derived fuel facility have been thermally treated with the addition of silicates [29]. Although this produced a dense black glass, the process was problematic, as the high treatment temperatures caused the evolution of significant volumes of HCl gas. The production of harmful gaseous emissions during vitrification can be minimised by washing APC residues prior to thermal treatment [30, 31]. APC residues can then be melted to produce a glass, and this product had potential uses as an aggregate in road bases [30].

Glass–ceramics can be produced from various silicate wastes by devitrification and powder sintering [14, 25, 32, 33]. Sintering has also been used to carry out preliminary investigations into the stabilisation of APC residues for safe disposal or possible reuse [3, 11]. Sintered pellets and powders were produced that had significantly improved retention of heavy metals, although the mechanical and other technical properties relevant to potential applications of these sintered materials were not reported. The thermal treatment of wastes to produce glass or glass–ceramics is an energy-intensive process, and it is necessary to reduce processing costs and produce materials with adequate physical properties to form products with commercial value [14].

This research has investigated for the first time the potential to develop new silicate glass–ceramic materials by sintering APC residues combined with other wastes. Electrostatic precipitator filter dust containing boron and soda-lime glass cullet have been used to tailor a suitable mix for sintering and glass–ceramic production, and the properties of the new materials have been compared to those of other similar materials and glass–ceramics.

Experimental procedures

Materials

APC residues from a major EfW plant in London, UK, which processes 420,000 tonnes of MSW per year, have been used in this work. This plant produces approximately 12,000 tonnes of APC residues each year. Representative samples were collected and stored in sealed plastic containers at room temperature. Figure 1 shows an SEM micrograph of as-received APC residues. The mean particle size of the APC residues was 35 μm with a range from 2 μm to 2 mm due to the presence of small pieces of partially combusted paper, which made up less than 1 wt%. The particle size was determined by laser diffraction (Mastersizer, Malvern Instruments).

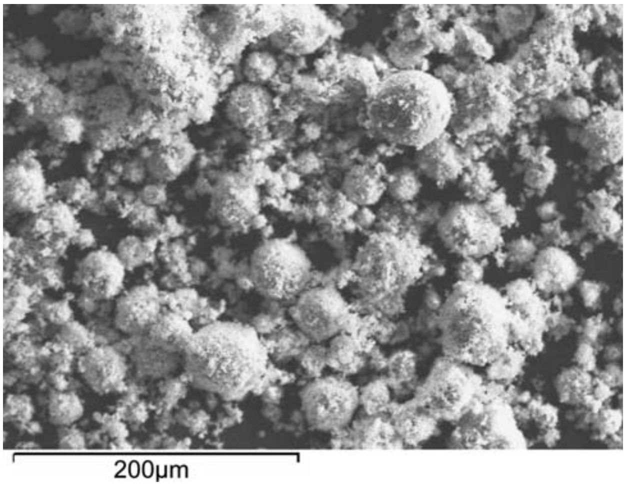

Fig. 1 SEM micrograph of as-received APC residues

Electrostatic precipitator (EP) dust is a hazardous waste (European Waste Catalogue number 19 04 02) generated from the production of textile fibreglass [5]. Flue gases from furnaces producing E-glass fibres contain acid components such as sulphur dioxide, boric acid and hydrofluoric acid. The gas is cleaned by scrubbing with lime; the precipitated dust is collected for disposal or recycling using either bag filters or electrostatic precipitators. This waste was selected for use in this research because it contains boron in the form of B_2O_3 which is used as a flux in glass production [34]. The as-received EP dust was crushed and ground using a Tema mill (Gy–Ro, Glen Creston Ltd.) for 2 min to give a powder with a mean particle size of 50 μm.

Soda-lime glass cullet was obtained from a glass recycling plant (Day Aggregates Ltd.). The cullet was crushed, washed, dried at 105 °C for 24 h and ground using the Tema mill to produce a powder with mean particle size of 30 μm.

Production of washed APC residues (WAPC)

APC residues were washed in distilled water for 2 h at a liquid-to-solid ratio of 20 which was selected based on results from a previous study [10]. The APC residues and distilled water were constantly stirred at room temperature during the washing procedure. The washed residues were separated from the wash water by vacuum filtration (Whatman 542 filter paper). The washed APC residues (WAPC) were dried for 24 h at 105 °C and crushed using a pestle and mortar to a mean particle size of 38 μm.

Characterisation of as-received materials, WAPC and wash water

The chemical composition and crystalline phases present in APC and WAPC residues, EP dust and glass cullet were determined using X-ray fluorescence analysis (Phillips 1606 XRF Spectrometer), inductively coupled plasma atomic emission spectroscopy (ICP-AES) (Thermo Electron IRIS Advantage ICP Spectrometer) and X-ray diffraction analysis (XRD, Philips PW1700 series automated powder diffractometer) using CuKα radiation with a secondary graphite crystal mono-chromator. The density of powders was determined using helium pycnometry.

The wash water generated from producing the WAPC sample was analysed by (ICP-AES) to determine the concentration of metals and by ion chromatography (Dionex ICS1000 Ion Chromatograph) for selected anions including Cl^-.

Production of sintered samples

Sintered samples were prepared with the compositions shown in Table 1. The proportion of WAPC residue was kept constant at 50 weight percent, and the EP dust and cullet proportions were systematically varied. The resulting powder mixes were milled using a tungsten carbide Tema mill (Gy–Ro, Glen Creston Ltd.) for 7 min to ensure homogenous mixing.

The homogenous powders were pressed using a steel die at a pressure of 124 MPa. In each case 0.5 g of powder was pressed to form compacts 9.5 mm in diameter and 3–4 mm high with a mean green density of 1.7 g/cm^3. These were sintered at a range of temperatures between 900 and 1,000 °C using a 2 h dwell time and a ramp rate of 10 °C/min in an electric furnace (Lenton). Samples were slowly cooled to room temperature within the furnace.

Table 1 Powder mixtures for sintering

Sample	Composition (wt%)		
	WAPC	Glass cullet	EP dust
S1	50	50	0
SB1	50	45	5
SB2	50	40	10
SB3	50	35	15
SB4	50	30	20

Characterisation of physical properties of sintered samples

The linear shrinkage was determined from the change in disc diameter that occurred during sintering. Sample density was determined using Archimedes principle. Average Vickers microhardness values were determined on polished surfaces of samples (Zwick Roell Indentec microindenter with a weight of 25 g) using at least ten indentations per sample.

Microstructural characterisation of sintered samples

Fractured and polished surfaces of selected samples were examined by scanning electron microscopy (Jeol JSM 840). Surfaces were polished using 1-μm diamond paste and gold coated. Crystalline phases present in powdered sintered samples were analysed using X-ray diffraction. A Philips PW1700 series automated powder diffractometer and CuKα radiation with a secondary graphite crystal mono-chromator were used.

Table 2 Chemical composition of APC residue, WAPC residue and EP dust

Element	Composition wt% (determined by XRF)		
	APC	WAPC	EP
Aluminium oxide	2.80	5.23	0.80
Calcium oxide	42	50.75	34
Carbon	2.13	N/A	0.47
Chloride	21	2.52	0.10
Chromium oxide	0.03	0.05	0.08
Copper oxide	0.40	0.90	0.03
Fluorine	0.13	N/A	2.20
Iron oxide	0.47	0.70	0.11
Potassium oxide	1.87	0.22	11.31
Magnesium oxide	0.05	0.09	0.32
Sodium oxide	2.68	0.60	4.14
Phosphorus pentoxide	0.78	1.09	0.05
Lead oxide	0.10	0.24	0.89
Silicon dioxide	7.14	10.15	2.96
Sulphur trioxide	5.66	5.51	10.88
Titanium dioxide	0.56	0.90	0.02
Boric oxide (by ICP-AES)	0.70	N/A	29.60
Zinc oxide	0.87	1.64	0.02
Loss on ignition (1,025 °C)	16.12	19.86	7.11

Results and discussion

Material characterisation

APC residues

Table 2 shows the chemical composition of APC residues. The major components are calcium oxide and chloride. The total Cl^- content is high compared to values reported for APC residues in other studies, and a more representative value for UK APC residues would be ~16 wt% [4, 9, 30, 35]. The data also indicate that a low percentage of SiO_2 is present. This primarily originates from entrained fly ash particles, and the low value indicates that it would probably not be possible to produce a glass from APC residues without the addition of glass-forming additives.

The XRD data shown in Fig. 2 indicate that the major crystalline phases present in APC residues are $Ca(OH)_2$, CaClOH, $CaCO_3$, KCl, NaCl and $CaSO_4$.

WAPC residues

Table 2 also shows chemical composition data for the WAPC residues. Washing removed up to 93% of the soluble chloride content (determined by ICP-AES analysis of the wash water). This compares favourably with earlier results, which concluded that the majority of chloride

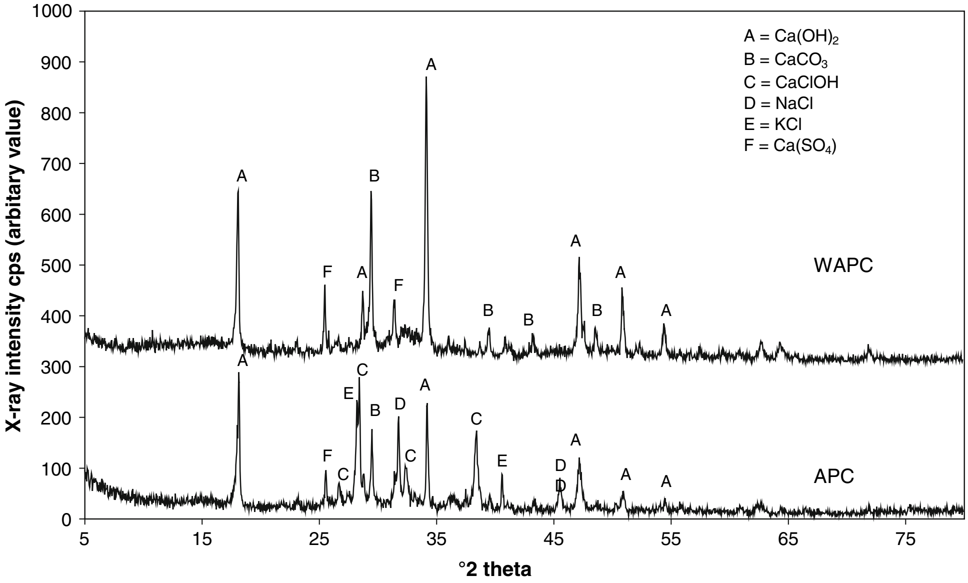

Fig. 2 X-ray diffractogram for as-received APC residue and WAPC residue

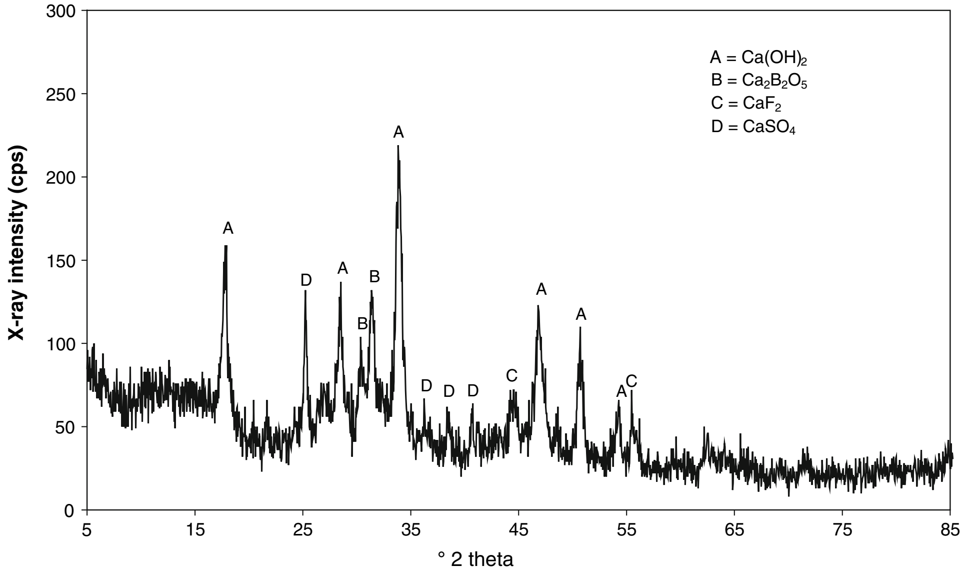

Fig. 3 X-ray diffractogram for EP dust

compounds could be readily removed [11, 12]. Although further work is required to optimise the washing procedure (in particular the reduction of wash water), producing low chloride APC residues is considered to be essential to limit hazardous gaseous emissions during subsequent thermal treatment. The production of a secondary waste is undesirable. However, the majority of the hazardous APC residues are incorporated into the sintered material and therefore diverted from the hazardous waste stream. It may be possible for the wash water to be used for neutralisation of other waste streams or precipitated to form a solid, and future research is needed to investigate such options.

The XRD data in Fig. 2 show that the major crystalline phases present in WAPC are $Ca(OH)_2$, $CaCO_3$, and $CaSO_4$, while the other phases, such as chlorides, present in the APC residues have been removed or are below detection limits.

Electrostatic precipitator (EP) dust

EP dust contains approximately 30 wt% boric oxide. Figure 3 shows the XRD trace of EP dust. It can be seen that boron is present as calcium borate ($Ca_2B_2O_5$). Fluorine is also combined with calcium as calcium fluoride (CaF_2). The high level of boric oxide is beneficial as it reduces the amount of EP dust that must be added to the batch mixes to achieve the possible flux and physical effects the borate may impart to the resulting glass–ceramic materials.

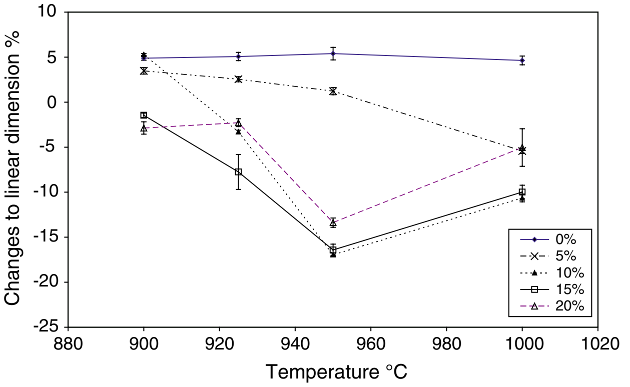

Fig. 4 Linear shrinkage versus sintering temperature (2-h dwell) for samples with different concentrations of EP dust

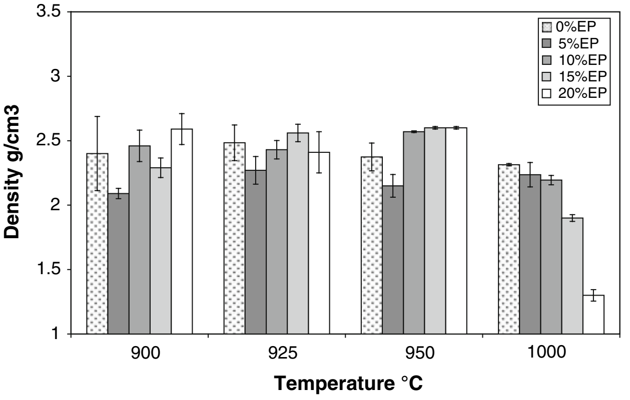

Fig. 5 Density versus temperature for sintered samples with different concentrations of EP dust

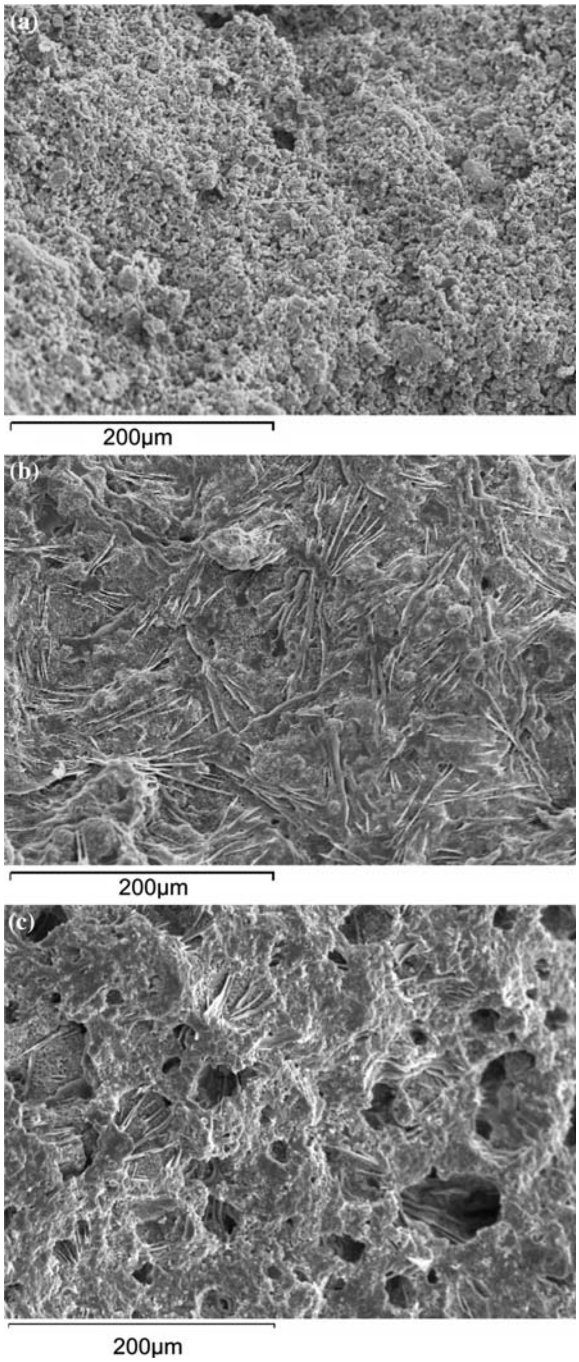

Fig. 6 SEM micrographs of fracture surfaces of sample SB2 sintered at (**a**) 900 °C; (**b**) 950 °C; (**c**) 1,000 °C for 2 h

Sintered samples containing WAPC residue

A temperature of 1,000 °C was required to sinter sample S1 (Table 1) which contained equal amounts of WAPC and glass cullet. In contrast, it was possible to produce fully sintered samples at 950 °C with the addition of EP dust.

Figure 4 shows the variation in linear shrinkage and expansion with sintering temperature. It can be seen that the addition of EP dust causes a significant increase in shrinkage. Sample SB1 did not exhibit such a strong trend as samples SB2-4, following a similar trend to that of S1, although with greater shrinkage.

Density versus sintering temperature data for samples with different concentrations of EP dust are shown in Fig. 5. Sintering at temperatures greater than 1,000 °C caused sample expansion due to bloating and a decrease in density. The samples containing EP dust showed a greater degree of linear shrinkage over the full range of sintering temperatures when compared to sample S1, which contained no EP dust. The low melting temperature (~970 °C) of EP dust promotes viscous flow and enhances densification of samples. Sample S1, containing no EP dust, remained relatively constant in linear dimensions as a result of sintering, but developed surface cracking at the edges and circumference.

As observed in Fig. 5 the general trend for all sintered samples containing EP dust was an increase in density with increasing temperature, up to an optimum temperature where maximum density was achieved. This was followed by a decrease in density as the optimum sintering temperature was exceeded. Sample SB1 exhibited a minor increase in density at optimum sintering temperature. The presence of EP dust can promote viscous flow during sintering, leading to increased densities of samples up to the optimum sintering temperatures.

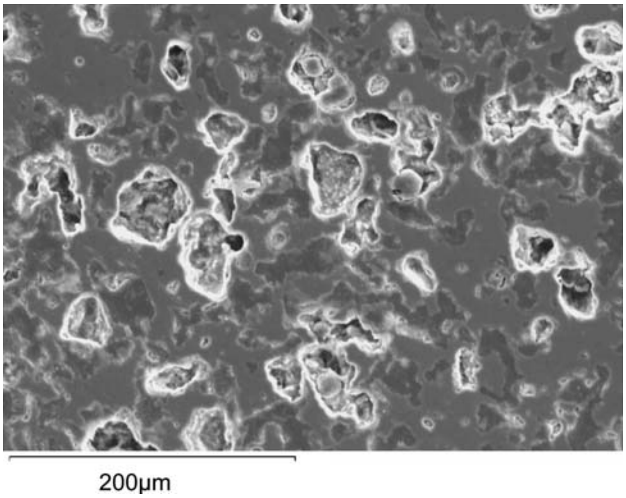

Fig. 7 SEM image of sample S1 sintered at 1,000 °C showing high porosity

Figure 6a–c shows the fracture surfaces of sample SB2 sintered at temperatures between 900 and 1,000 °C. It can

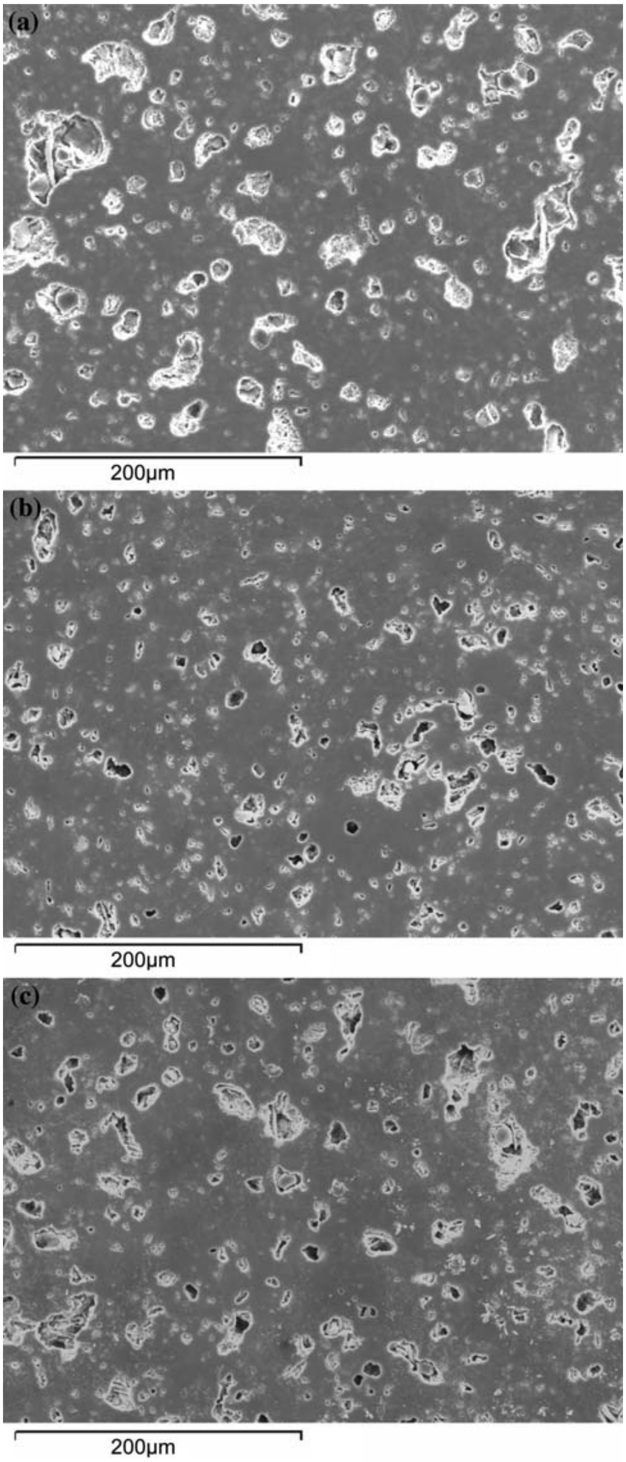

Fig. 8 SEM images of samples (**a**) SB2 (**b**) SB3 (**c**) SB4 sintered at 950 °C for 2 h, showing reduced porosity

be seen that sintering and associated densification occur over a relatively narrow temperature "window" of 100 °C, with 950 °C being optimum and bloating due to evolution of gases occurring at 1,000 °C. At 950 °C and above long, needle-like crystals are clearly visible, growing at random angles in a dense matrix. These crystals are also visible in the sample sintered at 1,000 °C, which also exhibits increased porosity.

SEM examination confirmed changes in porosity of sintered samples which occurred due to the addition of EP dust and temperature variation. Samples bloated when the firing temperature was too high for a particular batch mix, which caused pores to form within the sample, as visible in Figure 6c. Sample S1 was more porous than the samples containing EP dust due to decomposition of compounds forming gases with consequential pore formation within the body of the sample, as observed in Fig. 7. EP dust was a beneficial choice of additive in the present investigation involving APC residues as shrinkage and densification were enhanced during sintering.

Figure 8a–c confirms a reduction in porosity for samples SB2, SB3 and SB4 compared to S1 sintered at 950 °C. Comparison of only those samples containing EP dust shows that porosity was reduced up to an EP dust addition of 15 wt%. Above this value the porosity starts to increase. "Over-fluxing" of the mix may cause the increased production of phases of low viscosity, The increased level of EP dust is likely to result in increased gas evolution from compounds such as SO_3. The combination of these two phenomena can result in bloating of samples as evolved gases become trapped. The addition of 15 wt% EP dust or greater led to undesirable shape change of the sample apart from sintering shrinkage. The fully sintered samples SB3 and SB4 exhibited concave upper surfaces and sides. For this reason sinter batch mix SB2 was aesthetically superior to all other mixes. Minimal shape distortion of the part during sintering is essential if these materials are to find applications as construction products (e.g. floor tiles).

All samples sintered at optimum temperature formed wollastonite ($CaSiO_3$) and gehlenite ($Ca_2Al_2SiO_7$). XRD analysis confirmed that these phases were present, with minor variation in crystal size. An example of wollastonite and gehlenite crystal formation in an EP-containing sample is visible in Figure 6b for sample SB2, while XRD data of sample SB2 are presented in Fig. 9. The XRD analysis confirms that any chlorides present are below detection limits. The flattened, needle-like crystal structures present in the EP-dust-containing samples were not observed in sample S1 (without EP dust addition).

The Vickers microhardness values, presented in Table 3, show that the addition of EP dust improved the microhardness of sintered samples SB2-4. The lack of full crystal formation and higher porosity may explain the low microhardness of sample S1 and the high variation in values (standard deviation of 1.5 GPa) compared to samples SB2-4. Samples containing EP dust exhibit microhardness values up to 4.5 GPa which is similar to or greater than values obtained for sintered products from municipal waste incineration residues reported from other studies which ranged from 3.8 GPa to 6.7 GPa [25, 30, 32, 36–39]. In comparison, the microhardness of a typical commercially available porcelain stoneware tile is reported as 5.9 GPa [39]. This indicates that the present waste-derived glass–ceramics could be used as tiles for the construction sector. A high hardness leads to materials with improved wear and abrasion resistance. However other properties of the glass–ceramics need to be investigated for possible technical applications such as fracture toughness,

Fig. 9 X-ray diffractogram of sample SB2 sintered at 950 °C for 2 h showing wollastonite and gehlenite as main crystalline phase

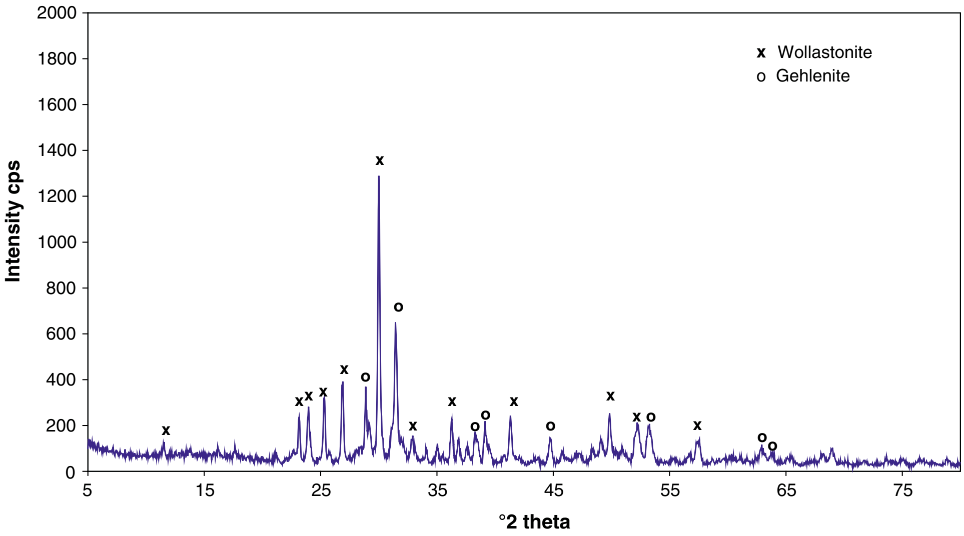

Table 3 Vickers microhardness values of sintered samples, sintered at the optimum sintering temperature for 2 h (Standard deviation: 0.3 GPa)

Sample	EP dust (wt%)	Microhardness (GPa)
S1	0	2.2 [1.5]
SB1	5	1.3 [0.5]
SB2	10	4.5 [0.7]
SB3	15	4.0 [1.0]
SB4	20	4.1 [0.8]

Standard deviations in square parentheses

thermal shock resistance and chemical durability (leaching resistance).

Conclusions

A simple water washing process will remove the majority of chloride compounds from as-received APC residue. This is an essential stage in any thermal-based treatment process as excessive chlorides produce noxious gaseous emissions during sintering of as-received APC residues.

The addition of electrostatic precipitator dust significantly reduces the firing temperature and causes enhanced linear shrinkage. Too high an EP dust content (>15 wt%) causes sample bloating and deformation, particularly at high sintering temperatures. Sintered samples containing optimum concentrations of EP dust (~10 wt%) exhibit improved hardness and densification.

The optimum sintering temperatures of the different samples lie within a narrow temperature range, outside which decreased densification is observed. Wollastonite and gelhenite crystalline phases were formed during sintering.

The high-density, structural integrity and adequate hardness values of sintered glass–ceramic products derived from washed APC residues mean that they have potential to be used in a range of construction products.

Acknowledgements This work was completed with financial support from EPSRC (UK) and Rio Tinto Minerals/Borax Europe Ltd through an Industrial Case Award from the Resource Efficiency Knowledge Transfer Network (KTN), formerly the Mini-Waste Faraday Partnership. The experimental assistance of staff and colleagues at Imperial College London and Rio Tinto Minerals (Guildford, UK) is greatly appreciated. Mr Peter Lewis is acknowledged for the provision of APC residue samples.

References

1. Environmental Services Association (2005) Draft APC residue case study, DEFRA, http://www.defra.gov.uk/environment/waste/hazforum/pdf/hwf-3-5iv.pdf, as on March 2005
2. Abanades S, Flamant G, Gagnepain B, Gauthier D (2002) Waste Manage Res 20(1):55
3. Lee PH, Nasserzadeh V, Swithenbank J, Laming JV, Goodfellow J, Mcleod C, Argent BB, Lawrence D, Garrod N (1999) Process Saf Environ Protect 77(B4):212
4. He P-J, Zhang H, Zhang C-G, Lee D-J (2004) J Hazard Mater B116:229
5. European Waste Catalogue (2000) In: 2000/532/EC
6. Geysen D, Vandecasteele C, Jaspers M, Wauters G (2004) J Hazard Mater 107(3):131
7. Alba N, Vazquez E, Gasso S, Baldasano JM (2001) Waste Manage 21(4):313
8. Todorovic J, Ecke H, Lagerkvist A (2003) Waste Manage 23(7):621
9. Barna R, Rethy Z, Imyim A, Perrodin Y, Moszkowicz P, Tiruta-Barna L (2000) Waste Manage 20(8):741
10. Rouchotas E (2001) MSc thesis, Department of Civil and Environmental Engineering, Imperial College London
11. Wang KS, Chiang KY, Lin KL, Sun CJ (2001) Hydrometallurgy 62(2):73
12. Chimenos JM, Fernandes AI, Cervantes A, Miralles L, Fernandes MA, Espiell F (2005) Waste Manage 25(7):686
13. Abbas Z, Moghaddam AP, Steenari BM (2003) Waste Manage 23(4):291
14. Boccaccini AR, Wu JP, Rawlings RD (2006) J Mater Sci 41(3):733. doi:10.1007/s10853-006-6554-3
15. Colombo P, Brusatin G, Bernardo E, Scarinci G (2003) Curr Opin Solid State Mat Sci 7(3):225
16. Boccaccini AR, Bucker M, Bossert J, Marszalek K (1997) Waste Manage 17(1):39
17. Barbieri L, Lancellotti I, Manfredini T, Queralt I, Rincon JM, Romero M (1999) Fuel 78(2):271
18. Olgun A, Erdogan Y, Ayhan Y, Zeybek B (2005) Ceram Int 31:153
19. Shao H, Liang K, Peng F, Zhou F, Hu A (2005) Minerals Eng 18(6):635
20. Catarino L, Sousa J, Martins IM, Vieira MT, Oliveira MM (2003) J Mater Process Technol 143:843
21. Pisciella P, Crisucci S, Karamanov A, Pelino M (2001) Waste Manage 21:1
22. Rozenstrauha I, Wu JP, Boccaccini AR (2005) Glass Technol 46(3):248
23. Yun YH, Yoon CH, Kim YH, Kim CK, Kim SB, Kwon JT, Kang BA, Hwang KS (2002) Ceram Int 28(5):503
24. Barbieri L, Corradi A, Lancellotti I, Pellacani GC, Boccaccini AR (2003) Glass Technol 44(5):184
25. Boccaccini AR, Schawohl J, Hern H, Schunck B, Rincon JM, Romero M (2000) Glass Technol 41(3):99
26. Boccaccini AR, Kopf M, Stumpfe W (1995) Ceram Int 21(4):231
27. Romero M, Rincon JM, Rawlings RD, Boccaccini AR (2001) Mater Res Bull 36(1–2):383
28. Rincon JM, Romero M, Boccaccini AR (1999) J Mater Sci 34(18):4413. doi:10.1023/A:1004620818001
29. Hollander HI, Plumley AL, Decesare RS (1996) J Hazard Mater 47(1–3):369
30. Kim JM, Kim HS (2004) J European Ceram Soc 24:2373
31. Wexell D, Vitrification of ash from waste-to-energy incinerators, Part II. Cold crown melting and parameters for scale-up, Pollution Prevention Resource Center Corning Inc., http://www.pprc.org/pprc/rpd/statefnd/nyschwm/vitrific.html, as on 05/08/2005,
32. Cheeseman CR, Monteiro Da Rocha S, Sollars C, Bethanis S, Boccaccini AR (2003) Waste Manage 23(10):907
33. Rawlings RD, Boccaccini AR (2004) Glass Technol 45(2):108
34. Borax Consolidated Limited (1965) In: Glasses, 3rd ed., London, Borax Consolidated London, p 83

35. Lundtorp K, Jensen DL, Sorensen MA, Christensen TH, Mogensen EPB (2002) Waste Manage Res 20(1):69
36. Cheeseman CR, Sollars CJ, Mcentee S (2003) Resour Conserv Recycl 40(1):13
37. Tsai C-C, Wang K-S, Chiou I-J (2006) J Hazard Mater 134(1–3):87
38. Romero M, Rawlings RD, Rincon JM (1999) J Eur Ceram Soc 19(12):2049
39. Esposito L, Tucci A, Naldi D (2005) J Eur Ceram Soc 25(9):1487